RESEARCH ARTICLE

Cathepsin W Is Required for Escape of Influenza A Virus from Late Endosomes

Thomas O. Edinger,[a,b] Marie O. Pohl,[a,b] Emilio Yánguez,[a] Silke Stertz[a]

Institute of Medical Virology, University of Zurich, Zurich, Switzerland[a]; Life Sciences Zurich Graduate School, ETH Zurich and University of Zurich, Zurich, Switzerland[b]

ABSTRACT   Human cathepsin W (CtsW) is a cysteine protease, which was identified in a genome-wide RNA interference (RNAi) screen to be required for influenza A virus (IAV) replication. In this study, we show that reducing the levels of expression of CtsW reduces viral titers for different subtypes of IAV, and we map the target step of CtsW requirement to viral entry. Using a set of small interfering RNAs (siRNAs) targeting CtsW, we demonstrate that knockdown of CtsW results in a decrease of IAV nucleoprotein accumulation in the nuclei of infected cells at 3 h postinfection. Assays specific for the individual stages of IAV entry further show that attachment, internalization, and early endosomal trafficking are not affected by CtsW knockdown. However, we detected impaired escape of viral particles from late endosomes in CtsW knockdown cells. Moreover, fusion analysis with a dual-labeled influenza virus revealed a significant reduction in fusion events, with no detectable impact on endosomal pH, suggesting that CtsW is required at the stage of viral fusion. The defect in IAV entry upon CtsW knockdown could be rescued by ectopic expression of wild-type CtsW but not by the expression of a catalytically inactive mutant of CtsW, suggesting that the proteolytic activity of CtsW is required for successful entry of IAV. Our results establish CtsW as an important host factor for entry of IAV into target cells and suggest that CtsW could be a promising target for the development of future antiviral drugs.

IMPORTANCE   Increasing levels of resistance of influenza viruses to available antiviral drugs have been observed. Development of novel treatment options is therefore of high priority. In parallel to the classical approach of targeting viral enzymes, a novel strategy is pursued: cell-dependent factors of the virus are identified with the aim of developing small-molecule inhibitors against a cellular target that the virus relies on. For influenza A virus, several genome-wide RNA interference (RNAi) screens revealed hundreds of potential cellular targets. However, we have only limited knowledge on how these factors support virus replication, which would be required for drug development. We have characterized cathepsin W, one of the candidate factors, and found that cathepsin W is required for escape of influenza virus from the late endosome. Importantly, this required the proteolytic activity of cathepsin W. We therefore suggest that cathepsin W could be a target for future host cell-directed antiviral therapies.

Influenza is a febrile respiratory disease of medical and economic importance in humans. The infectious agent of this disease, influenza A virus (IAV), is one of the best-studied viral pathogens. Nevertheless, certain aspects of the infectious cycle remain elusive. IAV belongs to the family *Orthomyxoviridae*, and it has a segmented negative-sense single-stranded RNA genome (1). The replication cycle of IAV starts with binding of the virus via its glycoprotein hemagglutinin (HA) to *N*-acetylneuraminic acid (sialic acid), a glycosylation motif on membrane proteins at the surface of the airway epithelium (2). Attachment to target cells is followed by internalization via clathrin- and non-clathrin-mediated endocytosis or macropinocytosis (3–5). Internalized particles are transported along the endosomal pathway, a complex cellular machinery, that mediates the turnover of early endosomes to late endosomes by fusion with lysosomal vesicles or proton influx and acidification (6, 7). IAV exploits the acidification of endosomes and fuses at low pH with the endosomal membrane (8,

9). This fusion of viral and endosomal membranes allows the delivery of viral genomes in the form of viral ribonucleoproteins (vRNPs) to the cytoplasm and their subsequent transport into the nucleus, the site of IAV genome replication (10, 11). While the functions of the viral proteins in the entry process are thought to be well understood, much less is known about the cellular proteins involved. However, such cellular factors could potentially be exploited as drug targets for host-directed antiviral therapy if they play a crucial role in IAV entry (12, 13). In order to reveal cellular factors required for IAV, genome-wide RNA interference (RNAi) screens have been performed (14–18). These screens have provided us with hundreds of candidate factors, but to date, only a few follow-up studies have been done.

In this study, we analyze the role of cathepsin W (CtsW) for IAV replication, since CtsW was discovered to be a required factor for IAV, and it has been suggested that CtsW is involved in IAV entry into cells in one of the RNAi screens (15). Cathepsins are

cysteine proteases of the papain superfamily that are involved in numerous cellular functions, such as regulation of apoptosis or establishment of inflammatory processes (19). CtsW, together with cathepsin F, belongs to a relatively new subgroup of F-like cathepsins which is distinct from the well-studied cathepsin B- and L-like subgroups (20). Cathepsins B and L were shown to be required for Ebola virus entry by cleaving the viral glycoprotein in the endosomal compartment (21). Moreover, inhibition of cathepsin L also resulted in inhibition of severe acute respiratory syndrome coronavirus (SARS-CoV) infection (22, 23), whereas cathepsin B has been implicated in entry of Nipah virus (24). In contrast to cathepsins B and L, nothing is known about the possible function of CtsW in viral infections. While cathepsins B and L are lysosomal enzymes, CtsW was found to localize predominantly to the endoplasmic reticulum (ER) in HeLa, COS-7, and natural killer (NK) cells (25, 26). Its high expression in CD8$^+$ T cells and NK cells and its upregulation by interleukin 2 (IL-2) also distinguish CtsW from the other members of the family (25). It was observed that CtsW is not needed for the effector function of these cells (26), so the question of the function of CtsW remains unanswered.

Using assays specific for distinct stages of IAV entry, we show here that CtsW plays a role in late endosomal escape of IAV and that its cysteine protease activity is needed for this function. This establishes CtsW as a novel host factor for entry of IAV and a potential drug target.

RESULTS

Cathepsin W is required for influenza A virus multicycle growth. Human cathepsin W (CtsW) was among the well-scoring hits identified in a genome-wide RNAi screen for host factors required for IAV replication, and it was suggested that CtsW could play a role in IAV entry (15). In order to confirm and extend these findings, we analyzed the impact of small interfering RNA (siRNA)-mediated CtsW knockdown on viral growth of IAV strain A/WSN/33 at different times postinfection (p.i.) (Fig. 1A). Depletion of CtsW using two different siRNAs (siCtsW #2 and siCtsW #3) was found to reduce titers of A/WSN/33 up to 100-fold compared to cells transfected with a nontargeting control siRNA (siSCR). Cells treated with siRNAs targeting either a subunit of the vacuolar ATPase (siVATPase) or the viral nucleoprotein (siNP) showed an almost complete block of replication. siCtsW-mediated reduction of viral titers was not limited to A549 cells, as we observed similar effects in Wi38 lung fibroblast cells (Fig. 1B). To check whether siCtsW treatment leads to a reduction in viral titers for multiple IAV strains, we performed infection experiments in siRNA-treated A549 cells with the highly pathogenic avian strain A/FPV/Dobson/34 (H7N7) and the human strain A/Hongkong/68 (H3N2) (Fig. 1C and D). Both viral strains showed a significant decrease in viral replication at all time points tested. To assess whether the observed inhibition was specific to IAV, we analyzed the impact of CtsW knockdown on replication of vesicular stomatitis virus (VSV). siCtsW treatment did not lead to a significant reduction in VSV titers at 18 h p.i. (Fig. 1E), suggesting that the requirement of CtsW is specific for IAV but independent of the cell line and IAV strain.

Endogenous amounts of CtsW in A549 or Wi38 cells were too low for detection in Western blots. Therefore, we tested the knockdown efficiencies of the different siRNAs by cotransfecting the siRNAs with a plasmid encoding CtsW and performed West-ern blot analysis 48 h after transfection. Both siRNAs against CtsW potently inhibited CtsW expression (Fig. 1F).

Cathepsin W is required for an early step in influenza A virus replication. Next, we evaluated the requirement of CtsW for early stages of IAV infection. Using an immunofluorescence-based read-out, we measured the amount of NP within cell nuclei of siRNA-transfected A549 cells at early time points of infection. At 48 h after siRNA transfection, cells were infected with A/WSN/33 at a multiplicity of infection (MOI) of 5 and 3 h p.i. NP was stained and analyzed by confocal microscopy. In control cells treated with siSCR, cell nuclei showed a clear signal of NP, whereas cells treated with siCtsW or the siVATPase control showed a drastic reduction in nuclear NP (Fig. 2A). To exclude off-target effects, we repeated this experiment using six different siRNAs targeting CtsW. For each of the siRNAs, the NP signal at 3 h p.i. within cell nuclei ($n >$ 200) was quantified, and we observed a strong decrease compared to siSCR-treated cells (Fig. 2B). All six siRNAs reduced the plasmid-based expression of CtsW substantially (Fig. 2C), suggesting that all of them are able to reduce endogenous levels of CtsW below optimal amounts for IAV. In addition, no impact on cell viability was observed for any of the siRNAs targeting CtsW (Fig. 2D). These data indicate that CtsW is required for an early step during the IAV replication cycle.

Cathepsin W is not required for attachment, internalization, and early endosomal trafficking of IAV. To further characterize the function of CtsW in IAV replication, we tested the impact of CtsW knockdown on the initial steps of the viral life cycle. First, we examined the effect of siRNA-mediated knockdown of CtsW on viral attachment and internalization using biotinylated IAV that can be visualized with Cy3-labeled streptavidin. A549 cells were transfected with the respective siRNAs, infected with biotinylated IAV for 60 min on ice, which allows attachment but prevents internalization, then fixed, and stained with Cy3-labeled streptavidin. Flow cytometric analysis of membrane-bound virus revealed no difference in the percentage of Cy3-positive (Cy3$^+$) cells between siSCR- or siCtsW-treated cells (Fig. 3A, samples labeled 0 min), indicating that viral attachment is not affected by CtsW knockdown. The signal was strongly reduced when cells were preincubated with unlabeled streptavidin before fixation and Cy3 staining (Fig. 3A, samples labeled 0 min + Strep), showing that the specific staining of membrane-bound virus can be blocked with unlabeled streptavidin.

A second set of samples was transferred to 37°C after the infection on ice to allow internalization of the virus. At 30 min after incubation at 37°C, the cells were either mock treated or incubated with unlabeled streptavidin, then fixed, and stained with Cy3-labeled streptavidin (Cy3-streptavidin). Pretreatment with streptavidin could only partially block the Cy3 signal, as internalized virus particles will be protected from unlabeled streptavidin (Fig. 3A, samples labeled 30 min + Strep). Therefore, the ratio of blocked to unblocked Cy3 labeling indicates the amount of internalized virus. As with the attachment, there was no significant difference between cells transfected with siSCR and siCtsW (Fig. 3A, bottom right graph). These data indicate that CtsW is not required for attachment or internalization of IAV.

After attachment and internalization, the virus is transported via the endosomal pathway through the cytoplasm. Endosomes can be differentiated using a set of molecular markers, such as the early endosomal antigen 1 (EEA1), which is a specific marker for early endosomes. To elucidate whether CtsW plays a role in early
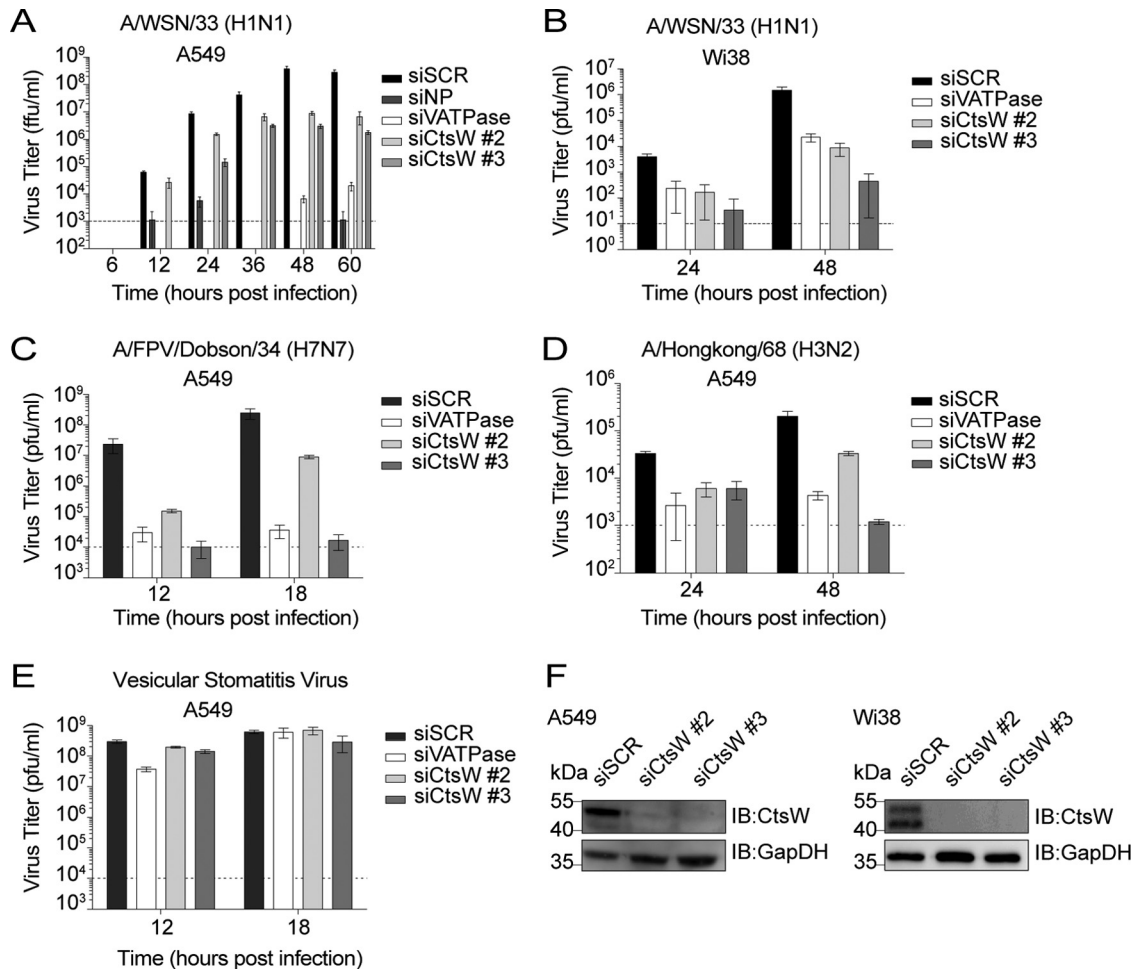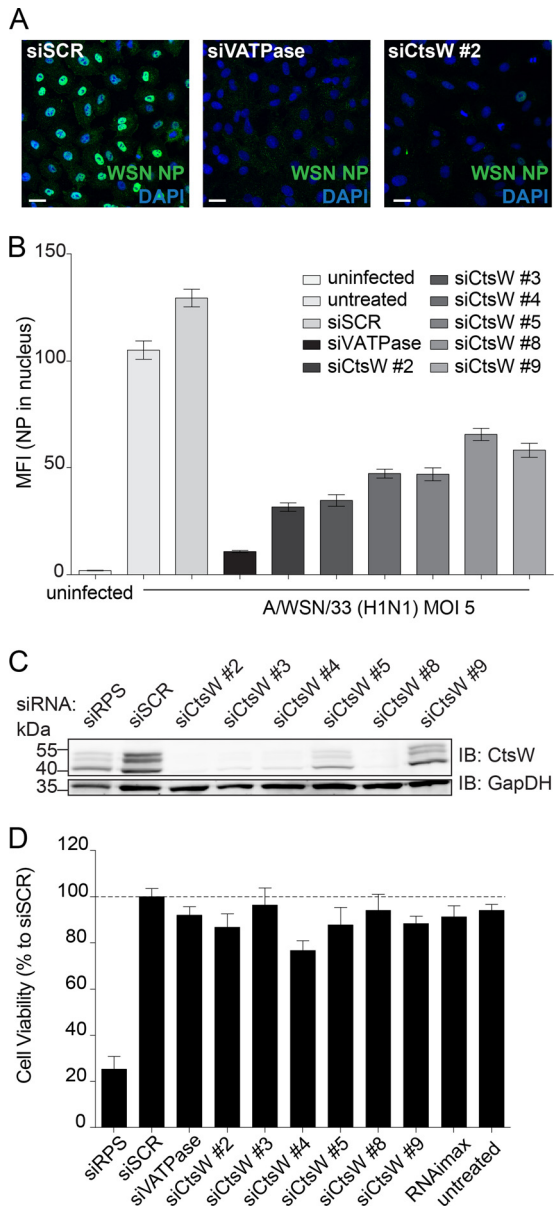
FIG 1 Cathepsin W is required for replication of different strains of IAV. (A) A549 cells were transfected with different siRNAs, and 48 h posttransfection, the cells were infected with A/WSN/33 (H1N1) at an MOI of 0.01. Supernatants were collected at the time points indicated on the x axis, and viral titers were determined by immunofluorescence-based titration on Vero cells. Virus titers were determined in focus-forming units per milliliter (ffu/ml). (B) Wi38 cells were transfected and infected as described above for panel A. Viral titers were determined by plaque assay. Virus titers were determined in plaque-forming units per milliliter (pfu/ml). (C and D) A549 cells were transfected with siRNAs, and 48 h posttransfection, the cells were infected with A/FPV/Dobson/34 (H7N7) at an MOI of 0.001 (C) or A/Hongkong/68 (H3N2) at an MOI of 0.1 (D). Supernatants were collected at the indicated time points, and virus titration was performed by plaque assay. (E) A549 cells were transfected with siRNAs, and 48 h after transfection, the cells were infected with vesicular stomatitis virus at an MOI of 0.001. At 12 to 18 h p.i., supernatants were analyzed for viral growth by plaque assay on Vero cells. (F) A549 or Wi38 cells were cotransfected with a plasmid encoding CtsW and two different siRNAs targeting CtsW or a nontargeting control siSCR. Efficiency of knockdown was analyzed by Western blotting (immunoblotting [IB]) using a mouse monoclonal anti-CtsW antibody and an antibody against glyceraldehyde-3-phosphate dehydrogenase (GapDH) as loading control. The positions of molecular mass markers (in kilodaltons) are indicated to the left of the blots. Panels A to E show representative results of at least two independent experiments, each experiment performed in triplicate. Values are means ± standard deviations (error bars).

endosomal trafficking, we transfected A549 cells with control siR-NAs or siRNAs targeting CtsW and infected these cells with A/WSN/33 at an MOI of 25. Viral infection was synchronized with a cold binding step at 4°C for 1 h. After the cold binding step, the inoculum was removed, the temperature was shifted to 37°C, and cells were fixed at different time points (15 to 180 min) p.i. To quantify the amount of viral NP in early endosomes, we performed immunofluorescence analysis for NP and EEA1 and measured the percentage of NP colocalizing with EEA1 using Imaris software. Between 15 and 180 min p.i., no difference in colocalization of NP with the early endosomal marker was observed in siSCR- or siCtsW-treated cells (Fig. 3B). Within the first 45 min p.i., a rapid increase in colocalization of NP and EEA1 was detected, and then colocalization declined, indicating a transient

presence of viral particles within the early endosomal compartment. Representative images from the 45-min time point illustrate the observed colocalization in both siSCR- and siCtsW-treated cells (Fig. 3C; see Fig. S1 in the supplemental material). This suggests that CtsW is not required for early endosomal trafficking and that presumably, a later step is affected by CtsW knockdown.

Cathepsin W is required for late endosomal escape of influenza A virus. Following the endosomal pathway, viral particles are transported from early to late endosomes, where they encounter low pH, which is required for fusion. To test whether CtsW is required for trafficking through late endosomes, we transfected A549 cells with siRNAs targeting CtsW or nontargeting control siRNA and infected these cells with A/WSN/33 at an MOI of 25. After an initial cold binding step of 1 h, the temperature was

FIG 2 Cathepsin W is required for an early step in the IAV replication cycle. (A) A549 cells were transfected with the indicated siRNAs, and at 48 h post-transfection, the cells were infected with A/WSN/33 (H1N1) at an MOI of 5. At 3 h p.i., cells were fixed and stained with a mouse monoclonal anti-NP antibody (green) and DAPI (blue) and analyzed by confocal microscopy. Bars, 20 μm. (B) This experiment was set up as described above for panel A. Nuclear NP signal was quantified by ImageJ software using the DAPI signal for region of interest (ROI) determination. Values are means of 200 cell nuclei per siRNA with standard errors of the means indicated by the error bars. MFI, mean fluorescence intensity. (C) Western blot for knockdown control was performed by cotransfection of a CtsW-encoding plasmid and siRNAs into A549 cells. At 48 h posttransfection, cell lysates were analyzed for CtsW protein expression by Western blotting using a mouse monoclonal anti-CtsW antibody and an antibody against GapDH as a loading control. (D) A549 cells were transfected with the indicated siRNAs. At 48 h posttransfection, cell viability was measured using the CellTiter-Glo luminescent cell viability assay. The experiment was performed in triplicate, and error bars represent standard deviations. In panels A to D, the results of one experiment that were representative of at least two independent experiments are shown.

shifted to 37°C to allow virus entry. Incubation at 37°C was stopped after 90 to 180 min p.i., and the cells were stained for NP and the late endosomal marker lysobisphosphatidic acid (LBPA) (27). We quantified the percentage of NP colocalizing with LBPA using Imaris software. As expected, in siSCR-treated cells, colocalization of NP and LBPA was observed up to 120 min p.i. (Fig. 3D). Of note, the observed colocalization was less pronounced than with the early endosomal marker, indicating a more rapid transport through the late endosomal compartment. At 180 min p.i., NP no longer colocalized with LBPA in control cells; at this time, NP was abundantly present within the nuclei of infected cells (Fig. 3E, top row; see Fig. S1 in the supplemental material). In contrast, cells treated with siCtsW displayed extended colocalization of NP with LBPA. We observed that a majority of the NP signal remained trapped in LBPA-positive compartments instead of trafficking to the nucleus as shown in the representative image of the 180-min p.i. time point (Fig. 3E, bottom row; Fig. S1).

To confirm that CtsW was required for incoming virions, we repeated the experiment in the presence of cycloheximide, which blocks translation and thus the synthesis of new NP. At 90 min p.i., we observed equal amounts of NP colocalizing with LBPA in both siSCR-transfected control cells and in siCtsW-transfected cells (Fig. 3F). In contrast, at 120 min and 180 min p.i., we detected more NP in LBPA-positive compartments in the siCtsW-transfected cells, whereas nuclear NP became detectable only in control cells (Fig. 3G; see Fig. S1 in the supplemental material). Taken together, these results suggest that CtsW is required for escape of IAV from late endosomes and/or transport of the RNPs to the nucleus.

To distinguish between these two possibilities, we next tested whether fusion of viral and endosomal membranes still occurs in the absence of CtsW. We generated a dual-labeled virus, which allowed us to measure fusion in a quantitative manner. IAV particles were labeled with two different dyes, one dye (R18 [octadecyl rhodamine B chloride] red) quenching the fluorescence of the other dye {DiOC [3,3′-dioctadecyl-5,5′-di(4-sulfophenyl)oxacarbocyanine] green}. If membrane fusion occurs, DiOC and R18 diffuse into the endosomal membrane, and quenching is no longer possible, which enables the detection of DiOC fluorescence. We infected siRNA-transfected A549 cells that were either pretreated with dimethyl sulfoxide (DMSO) or with bafilomycin A1, a known inhibitor of endosomal acidification and viral fusion. We synchronized infection by adding the virus in an initial 30-min cold binding step after which the temperature was shifted to 37°C to allow viral entry and fusion. At 90 min or 180 min p.i., cells were analyzed by confocal microscopy, and fusion sites were visible as bright green spots of DiOC fluorescence. These fusion sites (white arrowheads in Fig. 4A) were predominantly visible in siSCR-transfected control cells that were pretreated with DMSO. Both siCtsW- and siVATPase-transfected cells displayed fewer fusion sites as shown in representative images (Fig. 4A). We quantified the number of fusion sites using the spot detection algorithm of ImageJ and normalized to the number of cell nuclei (Fig. 4B). We observed two to six fusion sites per cell at 90 to 180 min p.i. in siSCR-transfected cells pretreated with DMSO. In contrast, no fusion sites were detected in siSCR-transfected cells pretreated with bafilomycin A1. Also, in siCtsW- and siVATPase-transfected cells, no or only a few fusion sites were observed, independent of their pretreatment with DMSO or bafi-
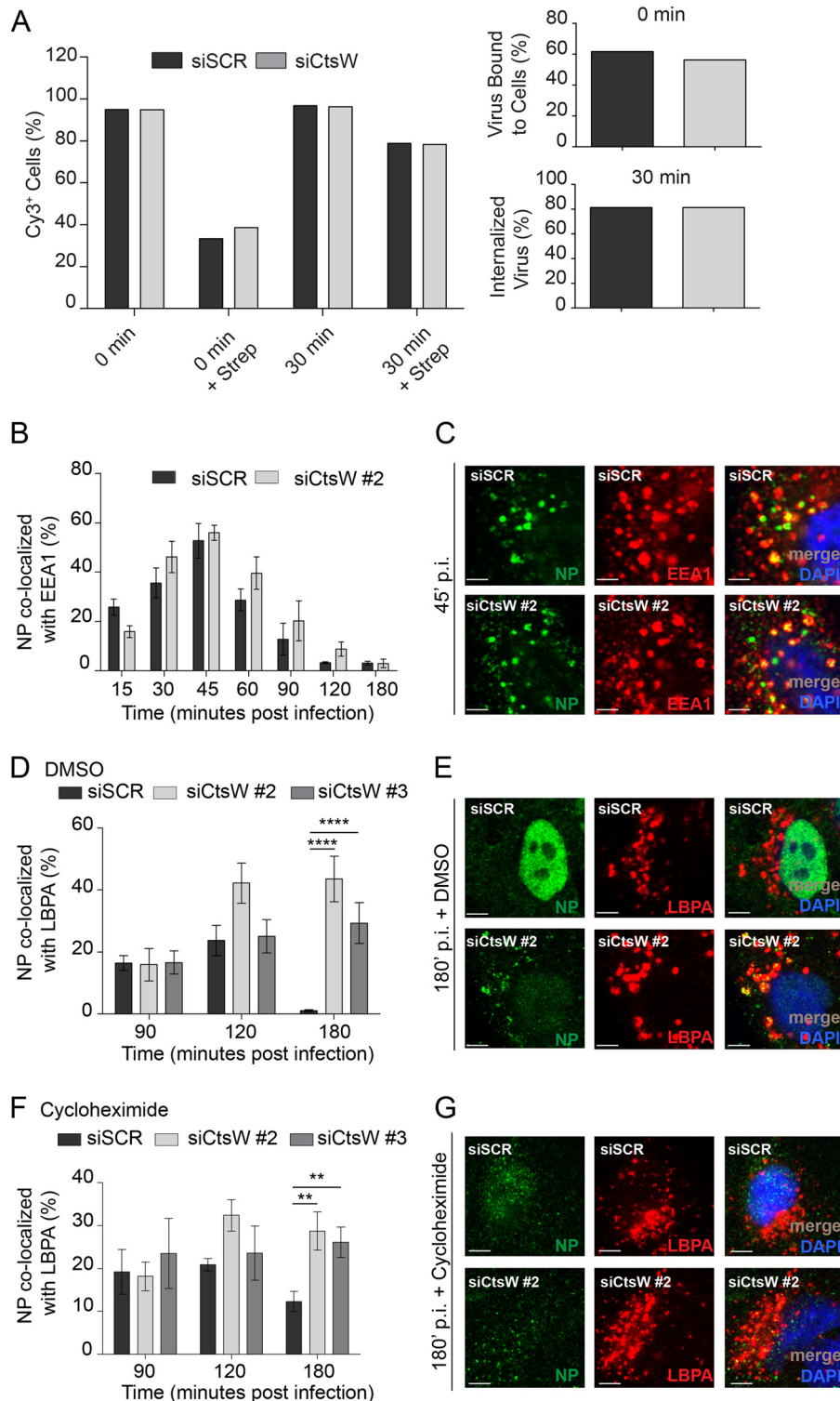
FIG 3 Knockdown of cathepsin W results in accumulation of NP in the late endosome. (A) A549 cells were transfected with siRNAs, and 48 h posttransfection, the cells were infected on ice with biotinylated A/WSN/33 for 1 h. Following attachment, the temperature was shifted to 37°C for 30 min or cells were directly fixed (samples labeled 0 min). Cells were treated with unlabeled streptavidin (samples labeled + Strep) or treated with PBS, then permeabilized and stained with Cy3-labeled streptavidin. Flow cytometry analysis was performed, and the relative amount of virus bound to cells was calculated by subtracting the percentage of Cy3-positive cells with streptavidin blocking from the percentage of Cy3-positive cells after PBS treatment (background subtraction). The relative amount of internalized virus was calculated as a ratio between the amount of virus-positive cells at 30 min plus streptavidin and the amount of virus-positive cells 30 min without streptavidin. (B to E) A549 cells were transfected with siRNAs, and 48 h later, the cells were infected with A/WSN/33 at an MOI of 25 for 1 h on ice. The inoculum was washed off, and the temperature was shifted to 37°C. Samples were fixed and permeabilized at the indicated time points. Cells were stained with a mouse monoclonal anti-EEA1 antibody (B and C) or mouse monoclonal anti-LBPA (D and E) (plus secondary anti-mouse antibody conjugated to Alexa Fluor

(Continued)

lomycin A1. This indicates that knockdown of CtsW results in inhibition of viral and endosomal membrane fusion.

The siCtsW-mediated inhibition of fusion in late endosomes raised the question whether CtsW localizes to late endosomal compartments. Although previous studies reported ER localization of CtsW (26, 28, 29), its production as an inactive precursor in the ER could mask its presence in other compartments. First, we analyzed the localization of CtsW by costaining of CtsW and the ER-resident chaperone calnexin in A549 cells stably expressing CtsW. As expected, a large amount of CtsW colocalized with the ER marker (Fig. 4C, top panel). Unfortunately, we were not able to costain for CtsW and the late endosomal marker LBPA, as both antibodies are derived from mice. We therefore costained for LAMP1 as a marker for late endosomes and observed a considerable amount of colocalization (Fig. 4C, bottom panels). Thus, in A549 cells, CtsW localizes to the ER but also at least partially to late endosomes where it could function to enable IAV fusion.

Cathepsin W is not required for acidification of endosomes or another late fusing virus. Next, we tested whether the inhibition of viral fusion upon knockdown of CtsW was due to changes in the pH of endosomes and a possible impact on acidification. To this aim, we treated siRNA-transfected A549 cells with lysotracker (LY), a dye that stains acidic compartments red fluorescent. As expected, cells treated with the VATPase inhibitor bafilomycin A1 did not display any lysotracker signal (Fig. 5A, bottom row). Cells transfected with siCtsW still displayed strong lysotracker staining that was indistinguishable from control cells (Fig. 5A, top row), suggesting that knockdown of CtsW does not drastically alter endosomal pH and thereby inhibit fusion. However, it is still possible that minor changes in pH that are not detectable with the lysotracker dye could contribute to the observed effects. We therefore tested the impact of CtsW knockdown on a strain of IAV, A/duck/Ukraine/1/1963, that has recently been shown to have a higher pH fusion optimum of pH 5.5 to 5.6 compared to pH 5.2 for A/WSN/33 (30). If reduced levels of CtsW resulted in slightly increased endosomal pH, this virus strain should display reduced sensitivity to knockdown of CtsW. We transfected A549 cells with control or CtsW-targeting siRNAs, infected the cells with virus at an MOI of 10, and quantified nuclear NP. We observed that A/duck/Ukraine/1/1963 replicated more slowly than A/WSN/33 did and that nuclear NP was detected only from 5 h p.i. onwards (data not shown). We therefore chose the 5-h time point to quantify nuclear NP. Similar to the results obtained with A/WSN/33, we detected a strong reduction in nuclear NP accumulation upon knockdown of CtsW (Fig. 5B; see Fig. S2A in the supplemental material). Next, we tested the impact of CtsW knockdown on lymphocytic choriomeningitis virus (LCMV), which also fuses in acidic compartments (31). Cells transfected with the control siSCR displayed robust viral replication in the cytoplasm of infected cells (Fig. 5C and Fig. S1B), whereas lower levels of viral NP were detected in cells transfected with siVATPase. In cells transfected with two siRNAs targeting CtsW, we could not detect any

significant changes in the cytoplasmic replication of LCMV, and therefore, we conclude that, although LCMV is a late fusing virus, it is not dependent on CtsW for fusion. These data suggest that CtsW does not impact endosomal pH, yet it is required for viral and endosomal fusion of IAV but not LCMV.

Cathepsin W does not cleave viral glycoproteins. Given that other cathepsin family members have been shown to proteolytically process viral glycoproteins (21, 22, 32, 33), we next tested whether CtsW cleaves IAV proteins on incoming virions. Since all previous experiments were performed with stocks of IAV that were grown in the presence of trypsin and thus contained HA1 and HA2 but no or negligible levels of HA0 (Fig. 5D), we did not expect to find a role for CtsW in cleavage of HA0 to HA1/HA2. However, additional cleavage events of hemagglutinin (HA) or neuraminidase (NA) could be possible. We infected A549 control cells or A549 cells overexpressing CtsW with A/WSN/33 (MOI of 50) for 1 h or 2 h. Cell lysates were prepared and tested for viral protein levels and for CtsW expression. Since we mapped the target step of CtsW to an event at or just before fusion in the late endosome, we did not expect NP or M1 matrix protein to be proteolytically processed by CtsW. Indeed, the levels of M1 and NP were unchanged upon overexpression of CtsW, and no lower-molecular-mass bands were observed (Fig. 5E; see Fig. S2C in the supplemental material). Interestingly, we also found similar levels of the two viral surface glycoproteins HA and NA (Fig. 5E and Fig. S2C), and we could not detect any cleavage products with a lower molecular mass for either protein. Thus, we assume that no CtsW-dependent cleavage of viral surface glycoproteins takes place.

The enzymatic activity of cathepsin W is required for influenza A virus entry. To test whether its catalytic activity as cysteine protease is required for the function of CtsW in IAV entry, we generated an enzymatically inactive mutant of CtsW, CtsW(C153A), by replacing cysteine at position 153, which is part of the catalytic triad by alanine. In addition, we introduced three silent mutations to achieve resistance to one of our siRNAs (CtsW #2) into both the wild-type CtsW- and CtsW(C153A)-encoding constructs. Both constructs were cloned into a lentiviral vector and used to generate stable cell lines expressing either CtsW (CtsW_res #2) or CtsW(C153A) (C153A_res #2). In addition, A549 cells were transduced with a lentivirus carrying no insert (control cells). To validate the cell lines, they were transfected with either siRNAs targeting CtsW or control siSCR, and lysates were analyzed by Western blotting for CtsW expression. As described above, endogenous levels of CtsW were not detected. In contrast, both cell lines transduced to express either wild-type CtsW or CtsW(C153A) showed robust expression of CtsW when transfected with siSCR or siCtsW #2 against which both constructs were made resistant (Fig. 6A). As expected, siCtsW #3 was still able to reduce CtsW levels below the limit of detection in Western blots, validating the generated cell lines. In addition, we also assessed growth of IAV in the cell lines overexpressing either wild-

Figure Legend Continued

546 [AF546]) and a rabbit anti-NP polyclonal serum (plus secondary anti-rabbit AF488). The amount of NP colocalizing with the respective marker was quantified using the standard colocalization function of Imaris software for at least 10 cells per condition (B and D). Representative images are shown in panels C and E. The values in panels B and D are mean percentages of NP colocalized with the marker ± standard deviations (error bars). Bars, 2 μm. (F and G) Same experimental setup as in panels B to E, but infection was performed in the presence of cycloheximide (100 μg/ml). The results of one experiment that were representative of two independent experiments are shown in panels A to G. (D to F) For significance testing, a two-tailed Student's t test was performed ($n \geq 10$). Values that are significantly different are indicated by bars and asterisks as follows: **, $P < 0.01$; ****, $P < 0.0001$.
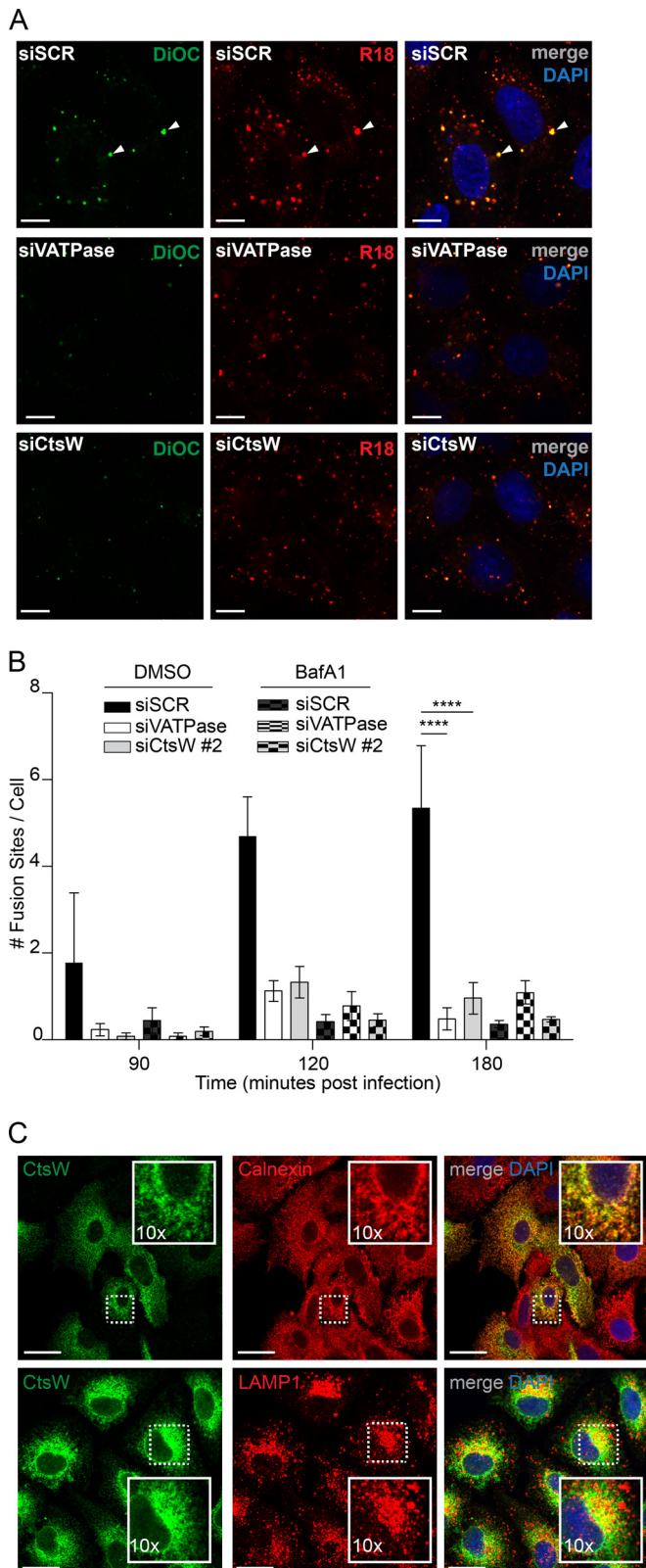
FIG 4 Knockdown of cathepsin W prevents fusion of viral and endosomal membranes. (A and B) A549 cells were transfected with siRNAs, and 48 h later, the cells were infected with a dual-labeled A/PR/8 virus (DiOC green and R18 red). Before the cells were infected, they were pretreated with DMSO or 10 nM bafilomycin A1 (BafA1) for 2 h. The virus was bound to cells for 30 min in a

(Continued)

type or mutant CtsW and found no difference in IAV replication (see Fig. S3 in the supplemental material). Next, we made use of the cell lines to assess whether the catalytic activity of CtsW was required for its function in IAV entry. After transfection of CtsW-targeting or control siRNAs, we infected these cells with A/WSN/33 at an MOI of 10. After an initial cold binding step, we allowed infection to proceed for 3 h at 37°C before we stained for IAV NP and measured the NP signal within the nuclei of infected cells. All three cell lines transfected with siSCR showed a clear NP signal in the nucleus at 3 h p.i. (Fig. 6B). As expected, the nuclear NP signal was strongly reduced in control cells upon knockdown of CtsW with either of the two siRNAs (Fig. 6B, top row). In contrast, CtsW_res #2 cells transfected with siCtsW #2 displayed a significantly higher NP signal due to the overexpression of siRNA-resistant CtsW. This effect was specific to siCtsW #2; transfection of siCtsW #3 still resulted in a strongly reduced nuclear NP signal (Fig. 6B, middle row). We could not observe a rescue of infection in the siCtsW #2-transfected cells when the cells were overexpressing catalytically inactive CtsW (Fig. 6B, bottom row). In addition, we transfected the cell lines with an siRNA targeting the VATPase subunit. Transduced cells, transfected with this siRNA, did not show any infection which shows that the observed rescue of infection is specific to CtsW knockdown. To verify these findings, we quantified the amounts of nuclear NP using ImageJ software. For siCtsW #2, rescue of infection by wild-type CtsW was highly significant compared to control cells, but expression of the inactive mutant did not increase the levels of nuclear NP significantly (Fig. 6C).

When staining the cell lines A549 CtsW_res #2 and A549 CtsW(C153A) _res #2 for CtsW by immunofluorescence, we observed that only about 60% of all cells were positive (data not shown). We hypothesized that this could be the reason for the incomplete rescue of infection by wild-type CtsW. Indeed, when we repeated the experiment but stained for CtsW and NP in parallel and quantified only nuclear NP from CtsW-positive cells, we observed an almost complete rescue of nuclear NP (Fig. 6D). Taken together, overexpression of CtsW can rescue the effect of siRNA-mediated knockdown of CtsW, showing that the observed impact on IAV entry is caused by depletion of CtsW levels rather than off-target effects of the siRNA. Moreover, the proteolytic activity of CtsW is required for its role in escape of IAV from late endosomes.

Figure Legend Continued

cold binding step (4°C), and then the cells were incubated for 90 to 180 min at 37°C to allow viral entry and fusion. Images were acquired by confocal microscopy without fixation and permeabilization of the samples. (A) Representative images from the 180-min p.i. time point are shown. The green spots in the siSCR DiOC panel and the white arrowheads indicate fusion sites. Bars, 10 μm. (B) Quantification of fusion sites was performed by spot analysis for the green DiOC signal using ImageJ software and 4× magnified images. Spot size was set at 20 pixels. The number of fusion sites was normalized to the number of cell nuclei. Values are mean numbers of fusion sites ± standard deviations (error bars). For significance testing, a two-tailed Student's *t* test was used ($n \geq 10$). Values that are significantly different are indicated by bars and asterisks as follows: ****, $P < 0.0001$. (C) A549 cells stably overexpressing CtsW were stained for CtsW with a mouse monoclonal antibody against CtsW and a rabbit polyclonal antibody against calnexin (top panels) or a rabbit polyclonal antibody against LAMP1 (bottom panels). Bars, 10 μm. In panels A to C, the results of one experiment representative of two independent experiments are shown.
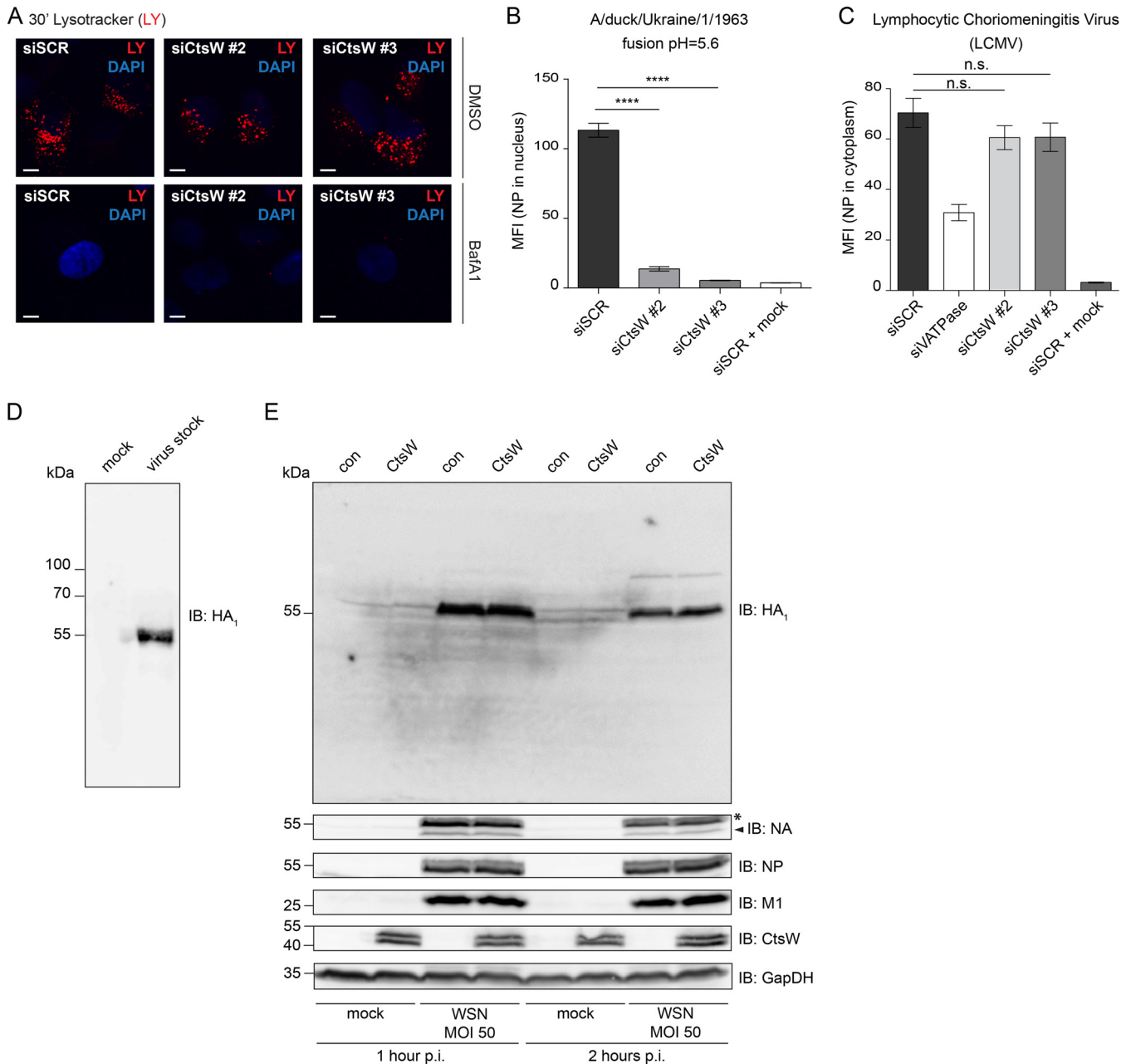
FIG 5 Cathepsin W is not required for acidification and does not cleave viral proteins. (A) A549 cells were transfected with the indicated siRNAs and either treated with DMSO or bafilomycin A1 for 2 h at 48 h posttransfection. Cells were then labeled with lysotracker DND-99 (red), and confocal images were acquired from unfixed samples. DAPI staining was introduced by the mounting medium. Bars, 5 μm. (B) A549 cells were transfected with siRNAs and infected with the indicated virus (MOI of 10) at 48 h posttransfection. Cells were fixed 5 h p.i., stained for viral NP using a mouse monoclonal NP antibody (plus secondary antibody anti-mouse AF488) and DAPI. Nuclear NP signal was quantified with ImageJ software. Mean values are shown with the standard errors of the means indicated by the error bars. Values that are significantly different by a two-tailed Student's t test are indicated by bars and asterisks as follows: ****, $P < 0.0001$ ($n \geq 100$). (C) A549 cells were transfected with siRNAs and infected with lymphocytic choriomeningitis virus (LCVM) at an MOI of 2 at 48 h posttransfection. Cells were fixed 7 h p.i., stained for LCMV NP using a mouse monoclonal LCMV NP antibody (plus secondary antibody anti-mouse AF488) and DAPI. Cytoplasmic LCMV NP signal was quantified with ImageJ software. Mean values are shown with the standard error of the mean indicated by the error bars. Values that are not significantly different ($P \geq 0.05$) by a two-tailed Student's t test are indicated (n.s.) ($n \geq 64$). (D) An aliquot of A/WSN/33 used in the previous experiments was lysed and prepared for SDS-PAGE, then viral proteins were separated on SDS-polyacrylamide gels and transferred by Western blotting, and HA was detected using a mouse monoclonal antibody specific for HA of A/WSN/33. Lysate of mock-infected A549 cells was run in parallel to control for specificity of the HA band. (E) A549 control cells (con) or CtsW-overexpressing cells were infected with A/WSN/33 (MOI of 50) for 60 min on ice and then transferred to 37°C for 60 or 120 min before they were lysed. Viral protein levels were analyzed by Western blotting using antibodies against HA, NA, NP, M1, CtsW, and GapDH as loading control. The asterisk marks the NP band visible above the NA band, as the blot was first stained for NP and subsequently for NA. In panels A to E, the results from one experiment representative of at least two independent experiments are shown.
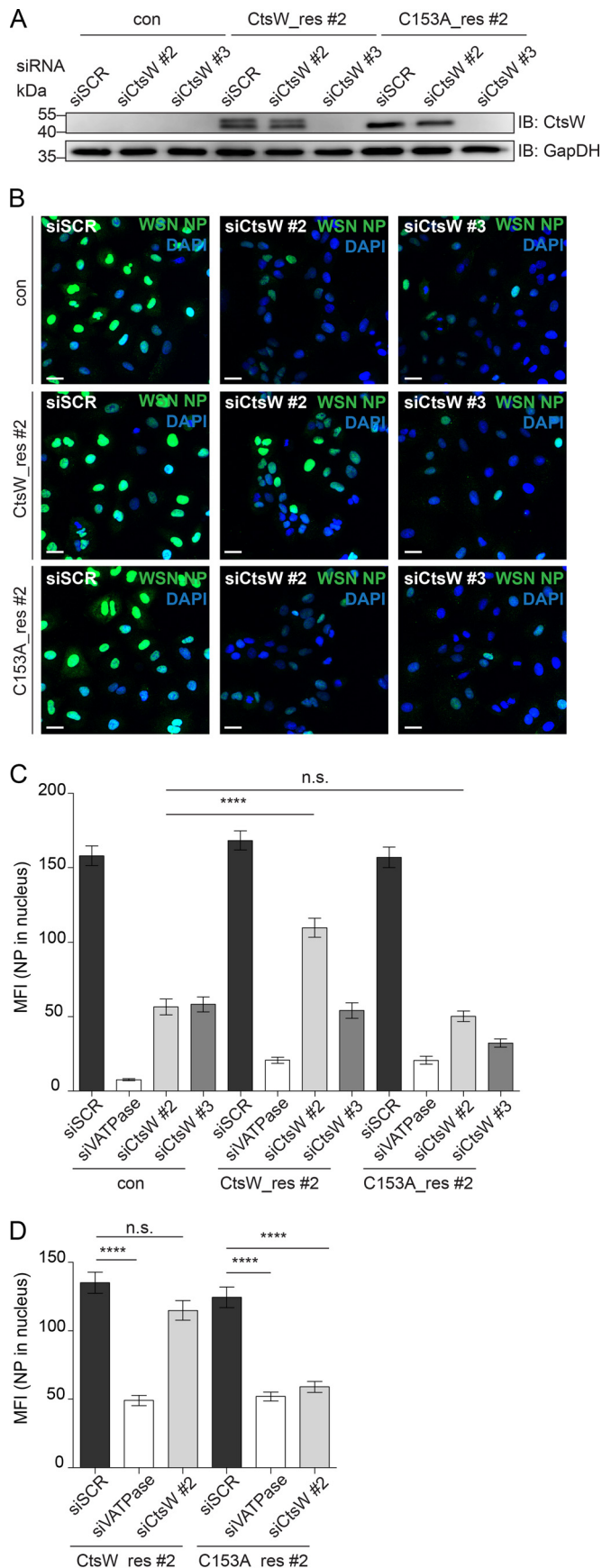
DISCUSSION

Genome-wide RNAi screens have discovered a plethora of cellular factors that influenza viruses hijack for their replication (14–18). The lists of identified factors hold great potential to reveal new aspects of the virus-host interplay and thereby uncover novel details about cellular processes. Moreover, such required cellular proteins represent potential drug targets, as shown by König et al. (15) and Stertz and Shaw (34). However, to date, there has been little follow-up on the identified factors, and so far, no promising drug target has emerged from the screens. In this study, we characterized CtsW, one of the hits identified in a genome-wide RNAi screen, and show that CtsW is required for fusion of influenza virus with the endosomal membrane and subsequent escape of IAV into the cytoplasm. The proviral function of CtsW required its catalytic activity, and therefore, we suggest that CtsW could be a potential drug target worth exploring for the development of novel antiviral agents.

Our data show that knockdown of CtsW by siRNAs leads to reduced virus titers for a number of different strains of IAV (Fig. 1). This was not due to off-target effects of the siRNAs, since six different siRNAs against CtsW resulted in the same phenotype (Fig. 2) and reintroduction of CtsW expression rescued the inhibition of IAV (Fig. 6). These data suggest a specific role for CtsW that cannot be compensated for by other cathepsins. In line with this hypothesis, we did not detect inhibition of IAV by inhibitors of cathepsin L and cathepsin B (data not shown).

We then mapped the step of the viral replication cycle that required CtsW and found that by 3 h p.i., the amount of nuclear NP was already strongly decreased upon CtsW knockdown (Fig. 2). Finer mapping of the target step revealed that virus attachment, internalization, and early endosomal trafficking were not affected. However, escape of IAV from the late endosome was blocked, and viral fusion was strongly inhibited upon CtsW knockdown (Fig. 3 and 4). We therefore conclude that CtsW is required for fusion or a step just before the fusion event. While we have a detailed understanding of the functions of the viral proteins in the fusion event (9), little is known about the cellular players involved. Early on, it was observed that low pH is required for fusion and that the endosomal VATPase complex is needed to

FIG 6 The catalytic activity of cathepsin W is required for IAV entry. (A) A549 cells were transduced using a lentiviral system to generate stable cell lines expressing wild-type CtsW (CtsW_res #2) or mutant CtsW(C153A) (C153A_res #2), both made resistant to siCtsW #2 by the introduction of three silent mutations into the target site of siCtsW #2. A549 cells transduced with a lentivirus carrying no insert were used as controls (con). Cells were transfected with siRNAs as indicated, and CtsW expression was assessed by Western blotting using a mouse monoclonal antibody against CtsW and an antibody against GapDH as loading control. (B and C) A549 control cells or cells stably expressing CtsW (wild type or mutant) were transfected with siRNAs targeting CtsW or a nontargeting control. At 48 h posttransfection, cells were infected with A/WSN/33 with an MOI of 10 for 3 h. Cells were stained using a mouse monoclonal anti-NP antibody (plus secondary antibody anti-mouse AF488) and DAPI. Representative images are shown in panel B. Bars, 10 μm. (C) Nuclear NP was quantified using ImageJ software. For significance testing, a two-tailed Student's t test was performed ($n = 150$). Values that are significantly different are indicated by bars and asterisks as follows: ****, $P < 0.0001$. Values that are not significantly different ($P \geq 0.05$) are indicated (n.s.). (D) Experimental setup as described above for panel B, but staining was performed using a rabbit polyclonal serum against NP and a mouse monoclonal antibody against CtsW. For quantification of nuclear NP, only cells expressing CtsW were included in the analysis. For significance testing, a two-tailed Student's t test was performed ($n \geq 90$). In panels A to D, the results of one experiment representative of three independent experiments are shown.

provide the low-pH environment in the endosome (8, 35, 36). Recently, the tetraspanin CD81 was identified as a second cellular player in the fusion process, but so far, we do not understand how CD81 exerts its function (37). With this study, we have identified a novel player in the fusion process, CtsW.

When analyzing the subcellular localization of CtsW, we found that a significant fraction of the CtsW staining colocalized with the ER-resident chaperone calnexin (Fig. 4). This is consistent with previous findings, which reported ER localization of CtsW (26, 28, 29). Interestingly, we also detected colocalization with a late endosomal marker (Fig. 4), and we therefore assume that at least a fraction of CtsW localizes to late endosomes. This would be consistent with a function of CtsW before or during the viral fusion process which takes place in the late endosome.

Notably, we detected two easily separable bands for CtsW on Western blots; the top band could sometimes be observed as a doublet. In contrast, only a single band could be detected for the catalytically inactive mutant. Thus far, we can only speculate that the additional bands represent modified forms, as this will require further studies. From results obtained with the catalytically inactive mutant (Fig. 6), we hypothesize that CtsW cleaves a yet unknown target in the late endosome and that this proteolytic cleavage event is important for fusion of the viral and endosomal membranes. This proteolytic cleavage event does not seem to impact endosomal pH. First, knockdown of CtsW did not result in detectable changes of the lysotracker signal, which marks acidic organelles (Fig. 5) (38). Second, a strain of IAV that had been shown to have a higher pH optimum for fusion (pH 5.5 to 5.6 versus pH 5.2 for A/WSN/33) was inhibited by knockdown of CtsW to an extent similar to that of strain A/WSN/33 (Fig. 5) (30). Instead, we hypothesize that the low pH is rather a requirement for CtsW function, as shown for other cathepsin family members (39, 40). The substrate that is cleaved by CtsW and then enables fusion to occur has yet to be identified. As we used trypsin-treated virus stocks for all experiments, we did not expect to find a role for CtsW in HA cleavage from HA_0 to HA_1 and HA_2. Moreover, strain A/FPV/Dobson/34 which contains a multibasic cleavage site in its HA protein was also sensitive to CtsW knockdown (Fig. 1). Therefore, we speculated that additional cleavage events could occur in HA or NA, but our experiments aiming to detect such cleavage events during the early stages of viral entry did not show any differences between control cells and cells overexpressing CtsW (Fig. 5). This could be indicative of cellular proteins being cleaved or degraded by CtsW, rather than viral proteins. However, we cannot exclude the possibility that a small fraction of a viral protein is targeted by CtsW but not detected by our Western blot setting.

In summary, this study establishes CtsW as a novel cellular factor required for entry of IAV into target cells at the stage of fusion between viral and endosomal membranes. The proteolytic activity of CtsW is needed for its proviral function and thereby presents a potential drug target for future development of new antivirals against influenza.

MATERIALS AND METHODS

Cells and viruses. A549 lung epithelial cells (ATCC CCL185), Wi38 lung fibroblast cells (ATCC CCL75), Vero, 293T (ATCC CRL 3216), and MDCK cells (ATCC CCL34) were grown in Dulbecco modified Eagle medium (DMEM) (Life Technologies) supplemented with 10% fetal calf serum and 1% penicillin-streptomycin (DMEM growth medium). Influenza A virus strains A/WSN/33 (H1N1), A/Hongkong/68 (H3N2), and A/duck/Ukraine/1/1963 (kindly provided by L. Hangartner, University of Zurich, Switzerland) were grown in 10-day-old embryonated chicken eggs; strain A/FPV/Dob-

son/34 (H7N7) was grown in Vero cells. Vesicular stomatitis virus (VSV) was grown in Vero cells. The titers of virus stocks were determined by plaque assay on MDCK or Vero cells. LCMV was kindly provided by S. Kunz, University Hospital of Lausanne, Lausanne, Switzerland)

Plasmids and antibodies. The expression construct pCAGGS-CtsW was generated by PCR amplifying the cDNA of CtsW from plasmid pCMV6-XL4-CTSW (CMV stands for cytomegalovirus) (catalog no. SC125558; Origene) using the forward primer 5′-GACAGAATTCACCATGGCACTGACTGCCCACC-3′ and reverse primer 5′-GACACTCGAGTCAGGGAGGGCAGGAGACTCGGGGC-3′ and cloning it into pCAGGS using EcoRI and XhoI. The plasmid pCAGGS-Flag-CtsW was constructed in the same way but using a different forward primer, 5′-GACAGAATTCATGGACTATAAGGACGACGACGACAAGGGGGTGGCACTGACTGCCCACC-3′. Next, three silent mutations were introduced into the cDNA of CtsW to make it resistant to knocking down by siCtsW #2 using a QuikChange mutagenesis kit (Agilent Technologies) and the following primers: forward, 5′-GGCCCCATCACCGTGACAATAAATATGAAGCCCCTTCAGC-3′, and reverse, 5′-GCTGAAGGGGCTTCATATTTATTGTCACGGTGATGGGGCC-3′. The catalytically inactive mutant CtsW(C153A) was also generated by using a QuikChange mutagenesis kit with the following primers: forward, 5′-CCAGAAAAACTGCAACTGCGCCTGGGCCATGGCAGCGGCAGGCA-3′, and reverse, 5′-TGCCTGCCGCTGCCATGGCCCAGGCGCAGTTGCAGTTTTTCTG-3′. The cDNAs of $CtsW_{siRes}$ and $CTSW(C153A)_{siRes}$ were amplified by PCR using the forward primer 5′-GACAGAATTCACCATGGCACTGACTGCCCACC-3′ and reverse primer 5′-GACATCTAGATCAGGGAGGGCAGGAGACTCGGGGC-3′, and the cDNAs were cloned into the lentiviral vector pLVX-IRES-puro (IRES stands for internal ribosomal entry site, and puro stands for puromycin) (catalog no. 632183; Clontech) with EcoRI and XbaI. The resulting constructs $pLVX$-$CtsW_{siRes}$-IRES-puro and $pLVX$-$CtsW(C153A)_{siRes}$-IRES-puro were verified by sequencing.

For Western blotting and immunofluorescence, the following primary antibodies were used: mouse monoclonal CTSW antibody (catalog no. WH0001521M1; Sigma-Aldrich), horseradish peroxidase (HRP)-conjugated glyceraldehyde-3-phosphate dehydrogenase (GAPDH) antibody (HRP conjugate [sc-25778; Santa Cruz]), mouse monoclonal M1 antibody (ATCC HB64), rabbit polyclonal NP antibody for Western blotting (kind gift of A. Nieto, Centro Nacional de Biotecnología, Madrid, Spain), rabbit polyclonal NP antibody for immunofluorescence (kind gift of P. Palese, Mount Sinai Hospital, NY, USA), mouse monoclonal HA antibody (41), rabbit polyclonal NA antibody (catalog no. PA5-32238; Thermo Scientific), mouse monoclonal EEA1 antibody (catalog no. 610457; BD Bioscience), mouse monoclonal LBPA [also called bis(monoacylglyceryl)phosphate (BMP)] antibody (catalog no. Z-PLBPA; Echelon Bioscience), mouse monoclonal LCMV NP antibody (kindly provided by S. Kunz, University Hospital of Lausanne, Lausanne, Switzerland), rabbit polyclonal calnexin antibody (catalog no. 22595; Abcam), rabbit polyclonal LAMP1 antibody (ab24170; Abcam), and a rabbit polyclonal Flag antibody (ab1162; Abcam).

Western blot analysis. For Western blot analysis, cells were lysed using Laemmli buffer (62.5 mM Tris-HCl [pH 6.8], 25% glycerol, 2% SDS, 350 mM dithiothreitol [DTT], 0.01% bromophenol blue), and lysates were run on 10 to 12% SDS−polyacrylamide gels. Proteins were transferred to a Hybond ECL nitrocellulose membrane (Fisher Scientific). Following transfer, the membrane was blocked by using 3% milk powder in Tris-buffered saline (TBS) supplemented with 0.05% Tween 20 (TBS-T). Primary and secondary antibodies were diluted in TBS-T with 3% milk powder and incubated with the membrane at room temperature (RT) for 1 to 2 h. Enhanced chemiluminescent (ECL) substrate (Thermo Scientific) was used for detection of protein bands.

DNA and siRNA transfection. All siRNAs were purchased from Qiagen and transfected using Lipofectamine RNAimax (catalog no. 13778-150; Life Technologies). A549 cells were reverse transfected with siRNA according to the manufacturer's protocol. The final concentration of all siRNAs was 30 nM. After 48 h, the transfection efficiency was controlled by cell death of

siRPS27A-treated cells. Cell viability was monitored using CellTiter-Glo luminescent cell viability assay (catalog no. G7570; Promega).

Plasmid transfection was performed using JetPrime (catalog no. 114-15; Polyplus) according to the manufacturer's protocol. Plasmid/siRNA cotransfection was performed using Lipofectamine 2000 (Life Technologies) as instructed by the manufacturer.

siRNA sequences. All siRNAs (Qiagen) were ordered with dTdT overhang and stored at −20°C. The sequences of the siRNAs are as follows (Qiagen catalog numbers shown in parentheses): scrambled1777 (custom siRNA), 5′-AAGCGTTCGTCCTATGATCGA-3′; siCtsW #2 (SI00025494), 5′-CACCGTGACCATCAACATGAA-3′; siCtsW #3 (SI00025501), 5′-CGCGTTC ATAACTGTCCTCAA-3′; siCtsW #4 (SI00025508), 5′-CCCAGCATGGGCAG AGAAATA-3′; siCtsW #5 (SI03079076), 5′-CCCGTGTGCAGAAACCGGAT A-3′; siCtsW #8 (SI05050577), 5′-CAGCCTGAATAAACCAAGACA-3′; siCtsW #9 (SI05050584), 5′-CAGCTCTGTCCTGTTAGGCCA-3′; siNP (custom siRNA), 5′-GGAUCUUAUUUCUUCGGAGTT-3′; siATP6V0C (SI04195590), 5′-CACAAAGTAGACCCTCTCCGA-3′; and siRPS27A (SI1027423), 5′-AAGCTGGAAGATGGACGTACT-3′.

Virus infection and titration. For virus infection of A549 or Wi38 cells, phosphate-buffered saline (PBS) was supplemented with 0.02 mM Mg^{2+}, 0.01 mM Ca^{2+}, 0.3% bovine serum albumin (BSA), and 1% penicillin-streptomycin and used to dilute virus stocks. The cells were washed once prior to infection, and the inoculum was either added at room temperature or on ice for 60 min to synchronize infection. The inoculum was removed and replaced by an appropriate amount of postinfection medium (DMEM supplemented with 0.3% BSA, 20 mM HEPES, and 1% penicillin-streptomycin). Cells were incubated for the indicated times at 37°C. Infectious titers of samples were determined by plaque assay on MDCK cells or by infecting A549 cells with serial dilutions of the samples and subsequent immunofluorescence staining of viral NP to quantify infectious virus.

Immunofluorescence staining and microscopy. For immunofluorescence staining, A549 cells were grown on glass coverslips in 24-well plates. Cells were fixed with 3% paraformaldehyde (PFA) and permeabilized using immunofluorescence (IF) buffer (PBS supplemented with 50 mM NH_4Cl, 0.1% saponin, and 2% BSA). After 1 h in IF buffer, the cells were incubated for 1 to 2 h at RT or overnight at 4°C with primary antibodies. After the cells were incubated with primary antibodies, they were washed three times with IF buffer before secondary antibodies were added for 1 to 2 h at RT. Alexa Fluor-conjugated donkey anti-mouse/rabbit antibodies (catalog no. A-21202, A-21206, A10036, and A10040; Life Technologies) were used as secondary antibodies. The cells were washed three times with IF buffer, before the coverslips were dipped in deionized water and inversely mounted onto glass microscope slides using DAPI (4′,6′-diamidino-2-phenylindole) Fluoromount G (catalog no. 0100-20; Southern Biotech).

All microscopy images were acquired with a confocal laser scanning microscope (Leica SP5). For colocalization analysis, the Imaris software with standard colocalization settings was used. Image processing and quantification of nuclear NP signal, as well as fusion site analysis, were performed using ImageJ software. Statistical analysis was done using PRISM software.

Attachment and internalization assay. The attachment and internalization assay was performed as previously described (42). Briefly, A/WSN/33 was concentrated over a sucrose cushion (30%) and biotinylated using the EZ-link NHS-SS biotin kit (Thermo Scientific). siRNA-transfected A549 cells were detached and cooled on ice in fluorescence-activated cell sorting (FACS) buffer (PBS supplemented with 2% BSA). Cells were infected on ice with biotinylated A/WSN/33 for 1 h and washed thoroughly with FACS buffer. Before the cells were incubated at 37°C for 30 min, they were incubated on ice either with FACS buffer containing unconjugated streptavidin (2 mg/ml; Life Technologies) or FACS buffer alone. Following internalization, the cells were either directly fixed with PFA (3%) or incubated with FACS buffer supplemented with streptavidin and sodium azide (0.1%) for 30 min and then fixed. For staining, Cy3-labeled streptavidin (Life Technologies) diluted in FACS buffer was used.

FACS analysis was performed on a CyAn ADP analyzer (Beckmann Coulter Inc.), and data were analyzed using FlowJo software.

Fusion assay. Measurement of viral fusion was performed according to a protocol previously described (43, 44). Briefly, IAV A/PR/8/34 was labeled using two fluorescent dyes, R18 (octadecyl rhodamine B chloride) and SP-DiOC18 [3,3′-dioctadecyl-5,5′-di(4-sulfophenyl)oxacarbocyanine] (Life Technologies), at a ratio of 1:2 with final concentrations of R18 of 22 μM and SP-DiOC18 of 46 μM. After intense vortexing for 60 min at RT, labeled virus was filtered through a 0.22-μm-pore-size filter. Virus was bound to cells for 30 min at a cold temperature (4°C), and after the cells were washed with PBS, the temperature was shifted to 37°C for 0, 90, or 180 min. Unfixed and unpermeabilized samples were mounted. Image analysis was carried out using the spot analysis function of ImageJ for SP-DiOC18 staining with a distinct spot size of 20 pixels and a subsequent correction for cell numbers.

Lysotracker. Lysotracker red DND-99 (catalog no. L7528; Life Technologies) was diluted in DMEM growth medium and added to cells at a final concentration of 25 nM. The cells were then incubated at 37°C for 30 min, washed once with medium, and mounted without fixation or permeabilization.

Lentivirus production and transduction of A549 cells. To produce lentiviral particles, 293T cells were transfected with pLVX-CtsW$_{siRes}$-IRES puro (wild type or mutant), a plasmid encoding VSV G protein (VSV-G), and an expression plasmid for HIV *gag-pol* using FuGene HD transfection reagent (Promega). Supernatants containing the lentiviral particles were harvested 48 h after transfection and supplemented with Polybrene (final concentration, 8 μg/ml). For transduction, A549 cells were seeded at low density, infected with the lentiviral particles, and kept at 37°C for 48 h. The medium was then changed to DMEM growth medium with 10 ng/ml puromycin. Selection was maintained during subsequent culture.

SUPPLEMENTAL MATERIAL

Supplemental material for this article may be found at http://mbio.asm.org/lookup/suppl/doi:10.1128/mBio.00297-15/-/DCSupplemental.

Figure S1, TIF file, 3.8 MB.
Figure S2, TIF file, 4.4 MB.
Figure S3, TIF file, 1.8 MB.

ACKNOWLEDGMENTS

REFERENCES

1. **Palese P, Shaw ML.** 2007. Orthomyxoviridae: the viruses and their replication, p 1647–1689. *In* Knipe DM, Howley (ed), Fields virology, **vol 2**, 5th ed. Lippincott Williams & Wilkins, Philadelphia, PA.

2. **Baum LG, Paulson JC.** 1990. Sialyloligosaccharides of the respiratory epithelium in the selection of human influenza virus receptor specificity. Acta Histochem Suppl **40**:35–38.

3. **Matlin KS, Reggio H, Helenius A, Simons K.** 1981. Infectious entry pathway of influenza virus in a canine kidney cell line. J Cell Biol **91**:601–613. http://dx.doi.org/10.1083/jcb.91.3.601.

4. **de Vries E, Tscherne DM, Wienholts MJ, Cobos-Jiménez V, Scholte F, García-Sastre A, Rottier PJ, de Haan CA.** 2011. Dissection of the influenza A virus endocytic routes reveals macropinocytosis as an alternative entry pathway. PLoS Pathog 7:e1001329. http://dx.doi.org/10.1371/journal.ppat.1001329.

5. **Sieczkarski SB, Whittaker GR.** 2002. Influenza virus can enter and infect cells in the absence of clathrin-mediated endocytosis. J Virol **76**:10455–10464. http://dx.doi.org/10.1128/JVI.76.20.10455-10464.2002.

6. **Lakadamyali M, Rust MJ, Babcock HP, Zhuang X.** 2003. Visualizing

infection of individual influenza viruses. Proc Natl Acad Sci U S A **100:**9280–9285. http://dx.doi.org/10.1073/pnas.0832269100.

7. **Mellman I.** 1996. Endocytosis and molecular sorting. Annu Rev Cell Dev Biol **12:**575–625. http://dx.doi.org/10.1146/annurev.cellbio.12.1.575.

8. **Maeda T, Ohnishi S.** 1980. Activation of influenza virus by acidic media causes hemolysis and fusion of erythrocytes. FEBS Lett **122:**283–287. http://dx.doi.org/10.1016/0014-5793(80)80457-1.

9. **Skehel JJ, Wiley DC.** 2000. Receptor binding and membrane fusion in virus entry: the influenza hemagglutinin. Annu Rev Biochem **69:**531–569. http://dx.doi.org/10.1146/annurev.biochem.69.1.531.

10. **Cros JF, Palese P.** 2003. Trafficking of viral genomic RNA into and out of the nucleus: influenza, Thogoto and Borna disease viruses. Virus Res **95:**3–12. http://dx.doi.org/10.1016/S0168-1702(03)00159-X.

11. **Martin K, Helenius A.** 1991. Transport of incoming influenza virus nucleocapsids into the nucleus. J Virol **65:**232–244. http://dx.doi.org/10.1016/0962-8924(92)90130-F.

12. **Edinger TO, Pohl MO, Stertz S.** 2014. Entry of influenza A virus: host factors and antiviral targets. J Gen Virol **95:**263–277. http://dx.doi.org/10.1099/vir.0.059477-0.

13. **Ludwig S.** 2009. Targeting cell signalling pathways to fight the flu: towards a paradigm change in anti-influenza therapy. J Antimicrob Chemother **64:**1–4. http://dx.doi.org/10.1093/jac/dkp161.

14. **Su WC, Chen YC, Tseng CH, Hsu PW, Tung KF, Jeng KS, Lai MM.** 2013. Pooled RNAi screen identifies ubiquitin ligase Itch as crucial for influenza A virus release from the endosome during virus entry. Proc Natl Acad Sci U S A **110:**17516–17521. http://dx.doi.org/10.1073/pnas.1312374110.

15. **König R, Stertz S, Zhou Y, Inoue A, Hoffmann HH, Bhattacharyya S, Alamares JG, Tscherne DM, Ortigoza MB, Liang Y, Gao Q, Andrews SE, Bandyopadhyay S, De Jesus P, Tu BP, Pache L, Shih C, Orth A, Bonamy G, Miraglia L, Ideker T, Garcia-Sastre A, Young JA, Palese P, Shaw ML, Chanda SK.** 2010. Human host factors required for influenza virus replication. Nature **463:**813–817. http://dx.doi.org/10.1038/nature08699.

16. **Karlas A, Machuy N, Shin Y, Pleissner KP, Artarini A, Heuer D, Becker D, Khalil H, Ogilvie LA, Hess S, Mäurer AP, Müller E, Wolff T, Rudel T, Meyer TF.** 2010. Genome-wide RNAi screen identifies human host factors crucial for influenza virus replication. Nature **463:**818–822. http://dx.doi.org/10.1038/nature08760.

17. **Brass AL, Huang IC, Benita Y, John SP, Krishnan MN, Feeley EM, Ryan BJ, Weyer JL, van der Weyden L, Fikrig E, Adams DJ, Xavier RJ, Farzan M, Elledge SJ.** 2009. The IFITM proteins mediate cellular resistance to influenza A H1N1 virus, West Nile virus, and dengue virus. Cell **139:**1243–1254. http://dx.doi.org/10.1016/j.cell.2009.12.017.

18. **Ward SE, Kim HS, Komurov K, Mendiratta S, Tsai PL, Schmolke M, Satterly N, Manicassamy B, Forst CV, Roth MG, García-Sastre A, Blazewska KM, McKenna CE, Fontoura BM, White MA.** 2012. Host modulators of H1N1 cytopathogenicity. PLoS One **7:**e39284. http://dx.doi.org/10.1371/journal.pone.0039284.

19. **Conus S, Simon HU.** 2008. Cathepsins: key modulators of cell death and inflammatory responses. Biochem Pharmacol **76:**1374–1382. http://dx.doi.org/10.1016/j.bcp.2008.07.041.

20. **Wex T, Levy B, Wex H, Brömme D.** 1999. Human cathepsins F and W: a new subgroup of cathepsins. Biochem Biophys Res Commun **259:**401–407. http://dx.doi.org/10.1006/bbrc.1999.0700.

21. **Chandran K, Sullivan NJ, Felbor U, Whelan SP, Cunningham JM.** 2005. Endosomal proteolysis of the Ebola virus glycoprotein is necessary for infection. Science **308:**1643–1645. http://dx.doi.org/10.1126/science.1110656.

22. **Simmons G, Gosalia DN, Rennekamp AJ, Reeves JD, Diamond SL, Bates P.** 2005. Inhibitors of cathepsin L prevent severe acute respiratory syndrome coronavirus entry. Proc Natl Acad Sci U S A **102:**11876–11881. http://dx.doi.org/10.1073/pnas.0505577102.

23. **Kawase M, Shirato K, van der Hoek L, Taguchi F, Matsuyama S.** 2012. Simultaneous treatment of human bronchial epithelial cells with serine and cysteine protease inhibitors prevents severe acute respiratory syndrome coronavirus entry. J Virol **86:**6537–6545. http://dx.doi.org/10.1128/JVI.00094-12.

24. **Diederich S, Sauerhering L, Weis M, Altmeppen H, Schaschke N, Reinheckel T, Erbar S, Maisner A.** 2012. Activation of the Nipah virus fusion protein in MDCK cells is mediated by cathepsin B within the endosome-recycling compartment. J Virol **86:**3736–3745. http://dx.doi.org/10.1128/JVI.06628-11.

25. **Wex T, Bühling F, Wex H, Günther D, Malfertheiner P, Weber E, Brömme D.** 2001. Human cathepsin W, a cysteine protease predominantly expressed in NK cells, is mainly localized in the endoplasmic reticulum. J Immunol **167:**2172–2178. http://dx.doi.org/10.4049/jimmunol.167.4.2172.

26. **Ondr JK, Pham CT.** 2004. Characterization of murine cathepsin W and its role in cell-mediated cytotoxicity. J Biol Chem **279:**27525–27533. http://dx.doi.org/10.1074/jbc.M400304200.

27. **Sun E, He J, Zhuang X.** 2013. Dissecting the role of COPI complexes in influenza virus infection. J Virol **87:**2673–2685. http://dx.doi.org/10.1128/JVI.02277-12.

28. **Wex T, Levy B, Smeekens SP, Ansorge S, Desnick RJ, Bromme D.** 1998. Genomic structure, chromosomal localization, and expression of human cathepsin W. Biochem Biophys Res Commun **248:**255–261. http://dx.doi.org/10.1006/bbrc.1998.8954.

29. **Wex T, Bühling F, Wex H, Günther D, Malfertheiner P, Weber E, Brömme D.** 2001. Human cathepsin W, a cysteine protease predominantly expressed in NK cells, is mainly localized in the endoplasmic reticulum. J Immunol **167:**2172–2178. http://dx.doi.org/10.4049/jimmunol.167.4.2172.

30. **Galloway SE, Reed ML, Russell CJ, Steinhauer DA.** 2013. Influenza HA subtypes demonstrate divergent phenotypes for cleavage activation and pH of fusion: implications for host range and adaptation. PLoS Pathog **9:**e1003151. http://dx.doi.org/10.1371/journal.ppat.1003151.

31. **Rojek JM, Kunz S.** 2008. Cell entry by human pathogenic arenaviruses. Cell Microbiol **10:**828–835. http://dx.doi.org/10.1111/j.1462-5822.2007.01113.x.

32. **Pager CT, Craft WW, Jr, Patch J, Dutch RE.** 2006. A mature and fusogenic form of the Nipah virus fusion protein requires proteolytic processing by cathepsin L. Virology **346:**251–257. http://dx.doi.org/10.1016/j.virol.2006.01.007.

33. **Pager CT, Dutch RE.** 2005. Cathepsin L is involved in proteolytic processing of the Hendra virus fusion protein. J Virol **79:**12714–12720. http://dx.doi.org/10.1128/JVI.79.20.12714-12720.2005.

34. **Stertz S, Shaw ML.** 2011. Uncovering the global host cell requirements for influenza virus replication via RNAi screening. Microbes Infect **13:**516–525. http://dx.doi.org/10.1016/j.micinf.2011.01.012.

35. **Daniels RS, Downie JC, Hay AJ, Knossow M, Skehel JJ, Wang ML, Wiley DC.** 1985. Fusion mutants of the influenza virus hemagglutinin glycoprotein. Cell **40:**431–439. http://dx.doi.org/10.1016/0092-8674(85)90157-6.

36. **White JM, Wilson IA.** 1987. Anti-peptide antibodies detect steps in a protein conformational change: low-pH activation of the influenza virus hemagglutinin. J Cell Biol **105:**2887–2896. http://dx.doi.org/10.1083/jcb.105.6.2887.

37. **He J, Sun E, Bujny MV, Kim D, Davidson MW, Zhuang X.** 2013. Dual function of CD81 in influenza virus uncoating and budding. PLoS Pathog **9:**e1003701. http://dx.doi.org/10.1371/journal.ppat.1003701.

38. **Dolman NJ, Kilgore JA, Davidson MW.** 2013. A review of reagents for fluorescence microscopy of cellular compartments and structures, part I: BacMam labeling and reagents for vesicular structures. Curr Protoc Cytom **Chapter 12:**Unit 12.30. http://dx.doi.org/10.1002/0471142956.cy1230s65.

39. **Guha S, Padh H.** 2008. Cathepsins: fundamental effectors of endolysosomal proteolysis. Indian J Biochem Biophys **45:**–75–90.

40. **Pillay CS, Elliott E, Dennison C.** 2002. Endolysosomal proteolysis and its regulation. Biochem J **363:**417–429. http://dx.doi.org/10.1042/0264-6021/3630417.

41. **Nohinek B, Gerhard W, Schulze IT.** 1985. Characterization of host cell binding variants of influenza virus by monoclonal antibodies. Virology **143:**651–656. http://dx.doi.org/10.1016/0042-6822(85)90407-6.

42. **Pohl MO, Edinger TO, Stertz S.** 2014. Prolidase is required for early trafficking events during influenza A virus entry. J Virol **88:**11271–11283. http://dx.doi.org/10.1128/JVI.00800-14.

43. **Sakai T, Ohuchi M, Imai M, Mizuno T, Kawasaki K, Kuroda K, Yamashina S.** 2006. Dual wavelength imaging allows analysis of membrane fusion of influenza virus inside cells. J Virol **80:**2013–2018. http://dx.doi.org/10.1128/JVI.80.4.2013-2018.2006.

44. **Banerjee I, Yamauchi Y, Helenius A, Horvath P.** 2013. High-content analysis of sequential events during the early phase of influenza A virus infection. PLoS One **8:**e68450. http://dx.doi.org/10.1371/journal.pone.0068450.